# Three-spin measurements in $pp \rightarrow pp$ at 730 MeV

M. W. McNaughton and S. Penttilä
*Los Alamos National Laboratory, Los Alamos, New Mexico 87545*

K. H. McNaughton and P. J. Riley
*University of Texas, Austin, Texas 78712*

D. L. Adams,* J. Bystricky,† E. Gülmez, and A. G. Ling‡
*University of California, Los Angeles, California 90024*
(Received 12 January 1990)

We have measured 14 spin observables for *pp* elastic scattering at 730 MeV and extracted the isospin-one amplitudes directly from the data. These new data complete the 730-MeV data set to the same standard as the 580-, 650-, and 800-MeV data.

## INTRODUCTION

Nucleon-nucleon (*NN*) scattering is important both as a direct test of strong interaction models and as a basic prerequisite for microscopic models of the nucleus. At intermediate energies the isospin-one (*pp*) data set is extensive. Arndt,[1] Bystricky,[2] and Bugg[3] maintain nucleon-nucleon data bases and produce phase-shift fits that may be accessed interactively via dial in or network connections to Clinton P. Anderson Meson Physics Facility (LAMPF), Virginia Polytechnic Institute and State University, and the University of Geneva.

Nevertheless, there are a few weak points in the data set. A few experiments contain unsuspected systematic errors which bias the phase shifts beyond the estimated uncertainty. Experience has shown that the uncertainties estimated from the phase-shift solutions are too optimistic until the data set is complete enough for a model-independent amplitude analysis. There are 5 complex *NN*-scattering amplitudes, so this requires approximately 10 independent spin measurements. According to this criterion the data are complete near 580 MeV (Ref. 4) and at 650 and 800 MeV.[5]

Near 730 MeV the phase shifts rely on an energy-dependent model to interpolate between a variety of data at different energies and angles. Lomon[6] studied the energy-dependent structure at intermediate energies and appealed for more data near this energy to clarify the $^3P_0$ phase shift. Lehar[7] has pointed out that the interpretation of the resonancelike loop in the $^3F_3$ phase shift depends on the detailed shape near 730 MeV and that this is not clearly determined by the existing data. The present measurements bring the 730-MeV data up to the standard of the 580-, 650-, and 800-MeV data.

Previous data are most conveniently accessed via Arndt's data base.[1] The diversity of notations is confusing, so Table I translates between the notations of Bystricky and Lehar,[8] the "Ann Arbor" convention[9] often used at LAMPF, and Arndt's notation. The new observables reported here are also defined in terms of the Bystricky and Lehar[8] notation in Table I. Briefly, the four suffixes $(n,k,s,0)$ denote the spin directions of the scattered proton, the recoil proton, the beam proton and the target proton (respectively); $\mathbf{k}$ is parallel to the momentum vector, $\mathbf{n}=\mathbf{k}_{\rm in}\times\mathbf{k}_{\rm out}$, $\mathbf{s}=\mathbf{n}\times\mathbf{k}$, and 0 denotes no spin. Within the energy range 706–750 MeV the previously measured observables (in addition to the cross section) are $A_{00n0}, A_{00nn}, A_{00kk}, A_{00sk}, D_{s0s0}, D_{s0k0}, D_{k0k0}, K_{0ss0}, K_{0sk0}, K_{0kk0}$. ($D_{n0n0}$ has also been measured at $90^\circ_{\rm c.m.}$ only.) The new data reported here remeasure four and add ten new observables to this data set.

TABLE I. Definition of the observables.

| Observable | Bystricky | Arndt | LAMPF |
|---|---|---|---|
| $A_{00n0}$ | $A_{00n0}=P_{n000}$ | $P$ | $A_N$ |
| $D_{n0n0}$ | $D_{n0n0}$ | $D$ | $D_{NN}$ |
| $D_{s0s0}$ | $D_{s0s0}$ | $R$ | $D_{SS}$ |
| $D_{s0k0}$ | $D_{s0k0}$ | $A$ | $D_{LS}$ |
| $D_{k0s0}$ | $D_{k0s0}$ | $RP$ | $D_{SL}$ |
| $D_{k0k0}$ | $D_{k0k0}$ | $AP$ | $D_{LL}$ |
| $A_{00st}$ | $A_{00sk}\cos\theta_t + A_{00ss}\sin\theta_t\cos\phi$ | $A0ST$ | |
| $A_{00kt}$ | $A_{00kk}\cos\theta_t + A_{00ks}\sin\theta_t\cos\phi$ | $A0KT$ | |
| $K_{s00t}$ | $K_{s00k}\cos\theta_t + K_{s00s}\sin\theta_t\cos\phi$ | $KS0T$ | |
| $K_{k00t}$ | $K_{k00k}\cos\theta_t + K_{k00s}\sin\theta_t\cos\phi$ | $KK0T$ | |
| $M_{s0nt}$ | $M_{s0nk}\cos\theta_t + M_{s0ns}\sin\theta_t\cos\phi$ | $MSNT$ | |
| $M_{n0st}$ | $M_{n0sk}\cos\theta_t + M_{n0ss}\sin\theta_t\cos\phi$ | $MNST$ | |
| $M_{n0kt}$ | $M_{n0kk}\cos\theta_t + M_{n0ks}\sin\theta_t\cos\phi$ | $MNKT$ | |
| $M_{k0nt}$ | $M_{konk}\cos\theta_t + M_{k0ns}\sin\theta_t\cos\phi$ | $MKNT$ | |

## EXPERIMENTAL METHOD

The measurement was made in the external proton beam of LAMPF. 733-MeV protons, polarized to about $P_b=0.77$ by the Lamb-shift ion source, were precessed by a solenoid and three dipoles into one of the three standard spin directions[8] $n$, $s$, or $k$ ($N,S,L$ in the Ann-Arbor notation[9]). The beam spin was reversed every 2 minutes to reduce systematic errors. All components of the beam polarization were monitored by a system of two beam line

 

polarimeters separated by a 29° bend. Beam intensity was measured by an ion chamber and by the summed counts in each polarimeter. After energy loss the average beam energy at the target center was 730 MeV.

The polarized proton beam was directed onto a polarized proton target (PPT) and the polarization of the scattered protons was measured with the Janus[10] polarimeter, as illustrated in Fig. 1. When setting the spin direction of the beam protons, allowance was made for the precession of the beam spin in the polarized target magnet. Scattered protons precessed both in the polarized target magnet and in the spectrometer magnet "Vartola."

The target material was propanediol doped with paramagnetic complex EHBA-Cr($V$) ($5\times10^{19}$ $e$/cm$^3$). The target was cooled in a dilution refrigerator and polarized dynamically in a horizontal magnetic field of 2.5 T to about $P_t=0.72$. The polarization was measured with an NMR method. The polarization measurements were calibrated with the thermal equilibrium polarization at about 1 K. The target polarization was reversed every few hours to cancel systematic errors.

The PPT magnet (a superconducting Helmholtz coil) was rotated to allow both scattered and recoil protons to be detected in wire-chamber detectors (Fig. 1). Consequently, the target spin direction $t$ had components in both the $k$ and $s$ directions, and some of the measured observables are linear combinations of the standard[8,9] observables.

Recoil protons passed between the PPT magnet coils (perpendicular to the magnetic field) and were detected by scintillator $S5$ and four multiwire drift chambers (Fig. 1). Scattered protons (emerging approximately parallel to the PPT magnetic field) were detected by scintillator $S1$ and multiwire proportional chambers $M1$, $M2$, $M3$, then

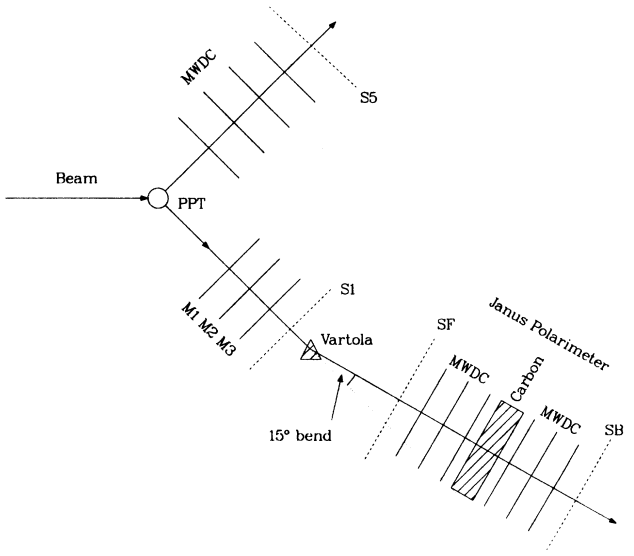


FIG. 1. Sketch of the experimental layout showing the polarized proton target (PPT), multiwire chambers ($M1$, *MWDC*, etc.), scintillators ($S1$, etc.) and the spectrometer magnet Vartola.

they were bent 15° either to the left or to the right by the spectrometer magnet Vartola, and finally they were analyzed by the carbon polarimeter Janus.[10] Vartola served both as a spectrometer magnet and as a spin precession magnet, precessing the proton spin by about ±45°. By combining the data with +45° and −45° precessions we extracted all three spin components $(n,s,k)$ for the scattered proton.

In principle, we made measurements with all three beam spins $(n,s,k)$, all three scattered proton spins $(n,s,k)$, and the target spin $t$. Therefore we measured observables of the form $X_{i0jt}$, where $i=(n,s,k,0)$ is the scattered proton spin, $j=(n,s,k,0)$ is the beam spin; the target spin $t$ is given in terms of the standard[8] unit vectors $\hat{\mathbf{k}}$ and $\hat{\mathbf{s}}$, and the polar and azimuthal angles $\theta_t$ and $\phi$ by

$$\hat{\mathbf{t}}=\hat{\mathbf{k}}\cos\theta_t+\hat{\mathbf{s}}\sin\theta_t\cos\phi$$

so that observables with the suffix $t$ are given by

$$X_{i0jt}=X_{i0jk}\cos\theta_t+X_{i0js}\sin\theta_t\cos\phi\ .$$

(The small azimuthal angle $\phi$ arises because the PPT magnet bends the incident protons out of the horizontal plane. Values of $\phi$ and $\theta_t$ are included in the tables.)

In practice, the beam spin was never set perfectly in the $n$, $s$, or $k$ directions so that every run measured some combination of many observables. The observables were therefore extracted by $\chi^2$ minimization. The average $\chi^2$ per degree of freedom was 1.1, indicating good internal consistency.

## ANALYSIS

Event-by-event data were digitized, read into a VAX750 computer via CAMAC and recorded on magnetic tapes. The tapes were replayed off line to reconstruct the proton tracks and extract the good $pp$ elastic events. Good events were selected by requiring good traceback to the target for both protons, good time of flight, and good opening angle and coplanarity for the two protons. Since the target traceback was taken from the wire chambers downstream of the spectrometer magnet, good target traceback implied good bend in the spectrometer.

Background from quasifree scattering from carbon in the target was examined by selecting events outside the elastic peaks, and was corrected for. Typical background was 1–2% of the signal; typical corrections were 0.001–0.002 to the asymmetries, which is very small in comparison with the uncertainties from counting statistics.

Yields for each spin state were corrected for beam intensity, system live time, and detector efficiency. Beam intensity was monitored using an ion chamber and independently using the summed counts in the beam-line polarimeters. Live time was monitored using several beam-related signals to sample the system busy signal; these were compared with the ratio of the number of events recorded by the computer to the number of event coincidences. Detector efficiencies were monitored using adjacent detectors to define a good event that should have fired the detector of interest. By examining internal con-

TABLE II. Spin observables (defined in Table I) for $pp$ elastic scattering at 730 MeV as a function of center-of-mass scattering angle $\theta$. All systematic uncertainties are included except for the overall normalization uncertainties (see the text).

| $\theta_{c.m.}$ | $\theta_t$ | $\phi$ | $A_{00n0}$ | $A_{00st}$ | $A_{00kt}$ | $D_{s0s0}$ | $D_{s0k0}$ | $D_{n0n0}$ |
|---|---|---|---|---|---|---|---|---|
| 38.4 | 23.0 | 15.4 | 0.527 | −0.230 | 0.242 | 0.715 | 0.208 | 0.874 |
| | | | ±0.008 | ±0.009 | ±0.009 | ±0.027 | ±0.026 | ±0.021 |
| 48.5 | 28.8 | 11.0 | 0.514 | −0.274 | 0.172 | 0.704 | 0.344 | 0.869 |
| | | | ±0.007 | ±0.009 | ±0.008 | ±0.022 | ±0.022 | ±0.018 |
| 59.5 | 34.6 | 8.8 | 0.459 | −0.310 | 0.184 | 0.597 | 0.329 | 0.818 |
| | | | ±0.008 | ±0.008 | ±0.008 | ±0.021 | ±0.020 | ±0.019 |
| 70.0 | 40.0 | 7.0 | 0.354 | −0.340 | 0.195 | 0.486 | 0.347 | 0.772 |
| | | | ±0.007 | ±0.008 | ±0.008 | ±0.017 | ±0.021 | ±0.019 |

| $D_{k0s0}$ | $D_{k0k0}$ | $K_{s00t}$ | $K_{k00t}$ | $M_{s0nt}$ | $M_{n0st}$ | $M_{n0kt}$ | $M_{k0nt}$ |
|---|---|---|---|---|---|---|---|
| −0.286 | 0.620 | −0.149 | 0.175 | −0.124 | −0.024 | 0.152 | 0.088 |
| ±0.030 | ±0.029 | ±0.017 | ±0.018 | ±0.036 | ±0.032 | ±0.031 | ±0.039 |
| −0.392 | 0.508 | −0.231 | 0.074 | −0.142 | −0.062 | 0.134 | −0.027 |
| ±0.024 | ±0.024 | ±0.014 | ±0.015 | ±0.031 | ±0.027 | ±0.028 | ±0.032 |
| −0.421 | 0.422 | −0.332 | 0.065 | −0.239 | 0.005 | 0.150 | 0.075 |
| ±0.025 | ±0.024 | ±0.013 | ±0.015 | ±0.031 | ±0.028 | ±0.027 | ±0.035 |
| −0.452 | 0.313 | −0.386 | 0.039 | −0.201 | −0.005 | 0.165 | −0.063 |
| ±0.022 | ±0.026 | ±0.011 | ±0.014 | ±0.028 | ±0.023 | ±0.030 | ±0.035 |

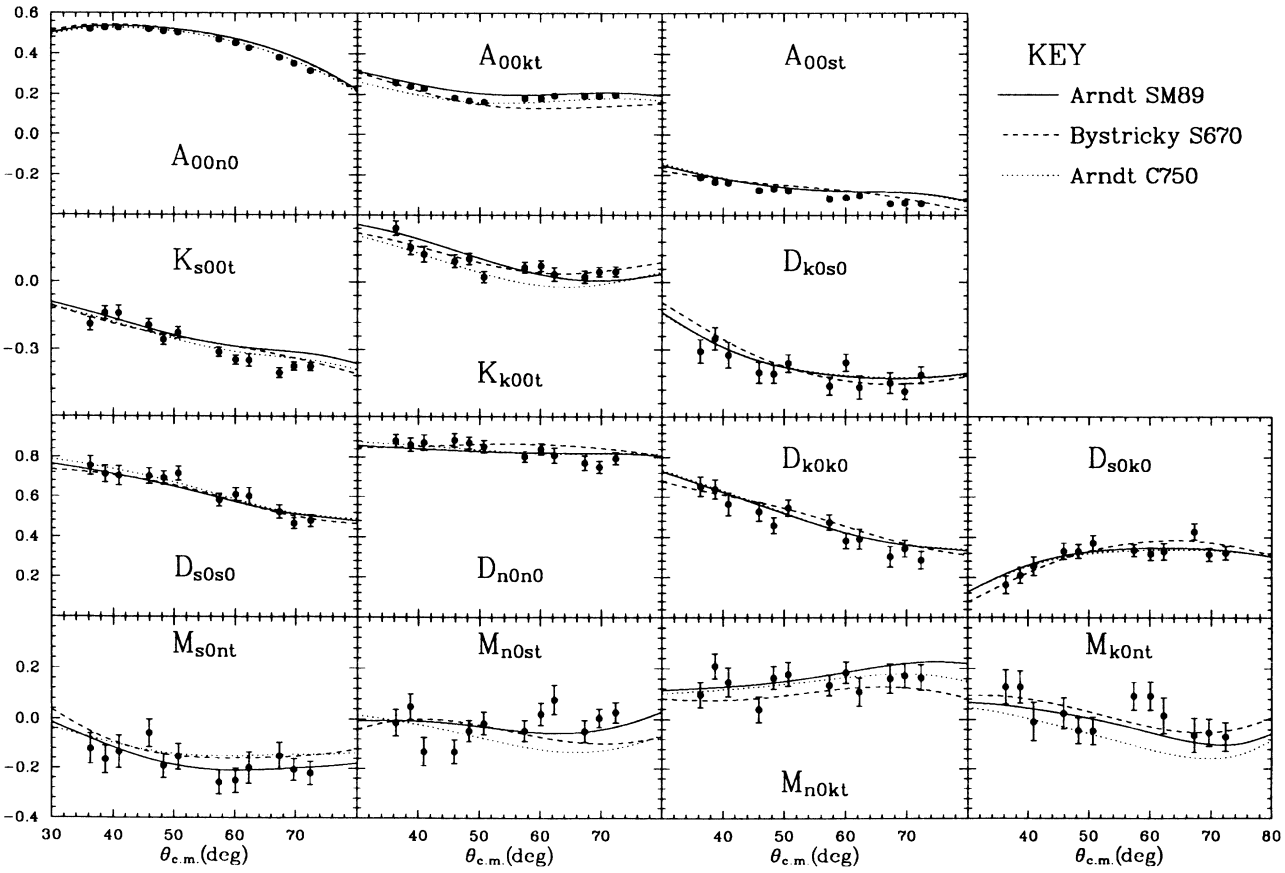


FIG. 2. Spin observables for $pp$ elastic scattering at 730 MeV compared with the phase-shift fit of Arndt and the phase-shift predictions of Bystricky.

TABLE III. The same data as in Table II, but rebinned into 12 center-of-mass angles $\theta$.

| $\theta_{c.m.}$ | $\theta_t$ | $\phi$ | $A_{00n0}$ | $A_{00st}$ | $A_{00kt}$ | $D_{s0s0}$ | $D_{s0k0}$ | $D_{n0n0}$ | $D_{k0s0}$ | $D_{k0k0}$ | $K_{s00t}$ | $K_{k00t}$ | $M_{s0nt}$ | $M_{n0st}$ | $M_{n0kt}$ | $M_{k0nt}$ |
|---|---|---|---|---|---|---|---|---|---|---|---|---|---|---|---|---|
| 36.3 | 23.0 | 16.7 | 0.521 | −0.212 | 0.258 | 0.755 | 0.162 | 0.881 | −0.307 | 0.652 | −0.189 | 0.241 | −0.122 | −0.015 | 0.096 | 0.128 |
| | | | ±0.008 | ±0.009 | ±0.009 | ±0.048 | ±0.044 | ±0.032 | ±0.052 | ±0.049 | ±0.030 | ±0.032 | ±0.062 | ±0.053 | ±0.050 | ±0.067 |
| 38.7 | 23.0 | 15.0 | 0.528 | −0.235 | 0.239 | 0.712 | 0.210 | 0.862 | −0.250 | 0.639 | −0.139 | 0.155 | −0.165 | 0.049 | 0.209 | 0.128 |
| | | | ±0.008 | ±0.009 | ±0.009 | ±0.043 | ±0.041 | ±0.033 | ±0.050 | ±0.047 | ±0.028 | ±0.031 | ±0.057 | ±0.051 | ±0.049 | ±0.064 |
| 40.9 | 23.0 | 14.4 | 0.528 | −0.240 | 0.230 | 0.704 | 0.256 | 0.872 | −0.324 | 0.565 | −0.140 | 0.125 | −0.134 | −0.132 | 0.146 | −0.009 |
| | | | ±0.008 | ±0.009 | ±0.009 | ±0.049 | ±0.047 | ±0.039 | ±0.058 | ±0.056 | ±0.033 | ±0.036 | ±0.066 | ±0.058 | ±0.057 | ±0.076 |
| 45.9 | 28.8 | 11.3 | 0.520 | −0.277 | 0.183 | 0.702 | 0.331 | 0.884 | −0.403 | 0.528 | −0.193 | 0.094 | −0.058 | −0.132 | 0.039 | 0.024 |
| | | | ±0.008 | ±0.010 | ±0.009 | ±0.040 | ±0.041 | ±0.033 | ±0.047 | ±0.046 | ±0.027 | ±0.029 | ±0.056 | ±0.049 | ±0.051 | ±0.061 |
| 48.3 | 28.8 | 10.9 | 0.510 | −0.269 | 0.169 | 0.692 | 0.330 | 0.871 | −0.409 | 0.459 | −0.257 | 0.104 | −0.191 | −0.047 | 0.163 | −0.044 |
| | | | ±0.008 | ±0.009 | ±0.009 | ±0.035 | ±0.035 | ±0.029 | ±0.040 | ±0.039 | ±0.023 | ±0.025 | ±0.049 | ±0.043 | ±0.045 | ±0.052 |
| 50.7 | 28.8 | 10.7 | 0.504 | −0.278 | 0.163 | 0.715 | 0.372 | 0.852 | −0.361 | 0.546 | −0.226 | 0.023 | −0.153 | −0.017 | 0.177 | −0.045 |
| | | | ±0.008 | ±0.009 | ±0.009 | ±0.036 | ±0.037 | ±0.030 | ±0.040 | ±0.041 | ±0.025 | ±0.026 | ±0.053 | ±0.045 | ±0.047 | ±0.055 |
| 57.4 | 34.6 | 8.8 | 0.470 | −0.318 | 0.179 | 0.581 | 0.336 | 0.802 | −0.463 | 0.474 | −0.312 | 0.065 | −0.257 | −0.047 | 0.134 | 0.092 |
| | | | ±0.009 | ±0.008 | ±0.008 | ±0.032 | ±0.031 | ±0.028 | ±0.039 | ±0.038 | ±0.021 | ±0.024 | ±0.048 | ±0.042 | ±0.041 | ±0.055 |
| 60.1 | 34.6 | 8.7 | 0.453 | −0.312 | 0.180 | 0.609 | 0.317 | 0.840 | −0.358 | 0.383 | −0.347 | 0.073 | −0.249 | 0.020 | 0.184 | 0.092 |
| | | | ±0.008 | ±0.008 | ±0.008 | ±0.033 | ±0.032 | ±0.029 | ±0.039 | ±0.039 | ±0.021 | ±0.024 | ±0.049 | ±0.044 | ±0.042 | ±0.056 |
| 62.3 | 34.6 | 8.9 | 0.429 | −0.303 | 0.194 | 0.601 | 0.329 | 0.809 | −0.469 | 0.391 | −0.349 | 0.035 | −0.198 | 0.076 | 0.108 | 0.015 |
| | | | ±0.009 | ±0.009 | ±0.009 | ±0.043 | ±0.042 | ±0.038 | ±0.052 | ±0.050 | ±0.028 | ±0.031 | ±0.064 | ±0.058 | ±0.055 | ±0.071 |
| 67.3 | 40.0 | 6.9 | 0.382 | −0.342 | 0.191 | 0.523 | 0.428 | 0.770 | −0.450 | 0.303 | −0.406 | 0.023 | −0.150 | −0.049 | 0.161 | −0.064 |
| | | | ±0.012 | ±0.008 | ±0.009 | ±0.033 | ±0.041 | ±0.036 | ±0.046 | ±0.052 | ±0.022 | ±0.028 | ±0.055 | ±0.044 | ±0.058 | ±0.069 |
| 69.7 | 40.0 | 7.0 | 0.353 | −0.339 | 0.191 | 0.466 | 0.314 | 0.749 | −0.488 | 0.343 | −0.376 | 0.045 | −0.206 | 0.004 | 0.172 | −0.054 |
| | | | ±0.008 | ±0.008 | ±0.009 | ±0.026 | ±0.033 | ±0.031 | ±0.035 | ±0.042 | ±0.018 | ±0.022 | ±0.044 | ±0.037 | ±0.048 | ±0.055 |
| 72.4 | 40.0 | 7.1 | 0.317 | −0.342 | 0.196 | 0.479 | 0.322 | 0.793 | −0.415 | 0.285 | −0.378 | 0.046 | −0.220 | 0.026 | 0.164 | −0.070 |
| | | | ±0.012 | ±0.008 | ±0.009 | ±0.029 | ±0.034 | ±0.031 | ±0.037 | ±0.044 | ±0.019 | ±0.023 | ±0.047 | ±0.040 | ±0.050 | ±0.058 |

sistency we estimate that each of these contribute an uncertainty of 0.004 to the asymmetries, and we have included these uncertainties in the results of Tables II and III.

Of the measured observables, the analyzing power $A_{00n0}$ is the most sensitive to possible systematic errors in beam intensity, live time and efficiency. So as an independent check we have extracted $A_{00n0}$ at $39.7^{\circ}_{\text{c.m.}}$ using only the beam line polarimeters and the method of Ref. 11 (which is unaffected by beam intensity, live time and efficiency). Using the polarimeter analyzing power[12] $=0.517\pm0.005$ and the correction for carbon quasifree scattering[11] $=1.024\pm0.003$ we calculate $A_{00n0}=0.529 \pm0.006$ at $39.7^{\circ}_{\text{c.m.}}$, in excellent agreement with the data in Tables II and III. We conclude that systematic errors from beam intensity, live time and efficiency are small.

The polarization of the scattered proton was measured by the Janus polarimeter using the standard procedures described in Ref. 10 and used in previous measurements at LAMPF.[13,14]

Data were taken for four $\theta$ settings of the spectrometer, and are presented in Table II for these four angles only. These data are averaged over the full angular acceptance of the spectrometer ($\pm2^{\circ}$ in the lab system). $A_{00n0}$ has been corrected by 0.002 for this acceptance, so that the values in Table II are point values at the angles quoted rather than averages over $\pm2^{\circ}$. Angular acceptance corrections for all other cases are negligible.

In Table III we give three $\theta$ bins for each spectrometer setting, i.e., a total of twelve values of the scattering angle $\theta_{\text{c.m.}}$. The advantage of Table II (with four values of $\theta_{\text{c.m.}}$) is the simplified bookkeeping for the target angles $\theta_t$ and $\phi$. These angles may be approximated in terms of the lab-system scattering angles $\theta_1$ for the scattered proton and $\theta_2$ for the recoil proton, as used by Bystricky and Lehar[8] in the expressions for the amplitudes. A negligible error of 0.001 or less in the observables is introduced by making the approximations

$$\sin\phi \approx 0.075/\tan\theta_1$$

and

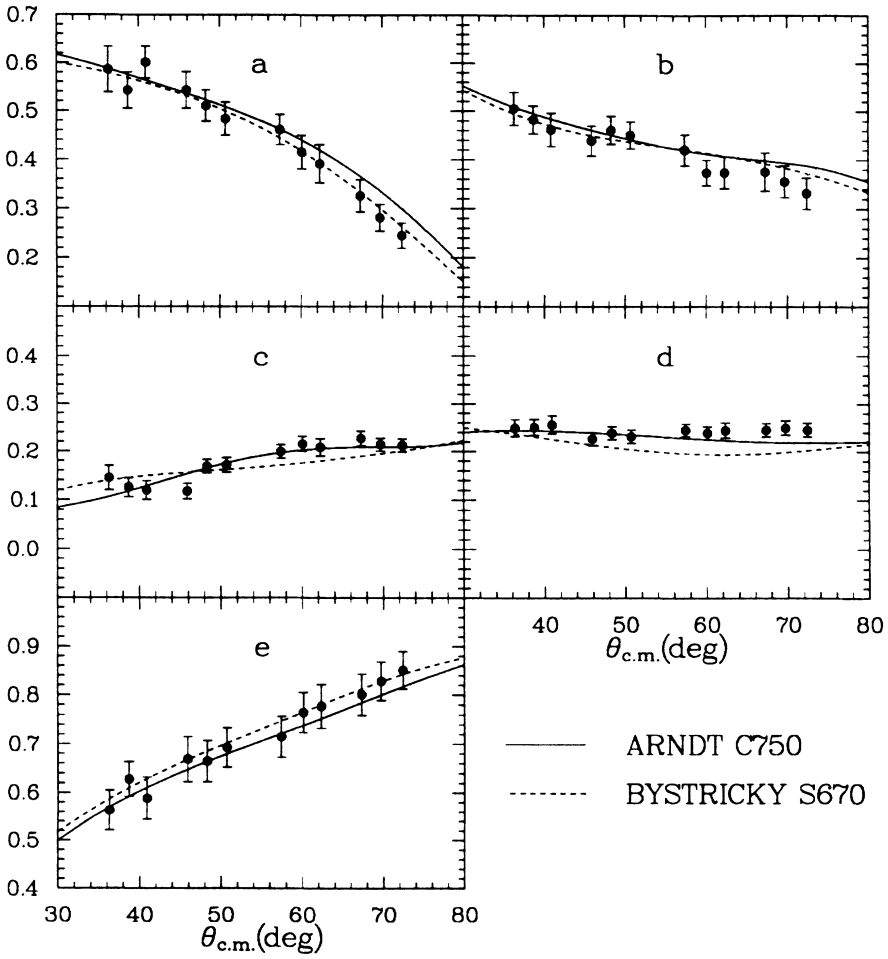


FIG. 3. Magnitudes of the *NN* isospin-1 amplitudes; direct reconstructions from the data compared with values from the phase shifts of Arndt and Bystricky.

$$\theta_t \approx 90° - \theta_2 + 0.7° .$$

For example, when $\theta_{\text{c.m.}} = 38.4°$ then $\theta_1 = 16.5°$ and $\theta_2 = 67.7°$ from kinematics. The approximations give $\phi = 14.7°$ and $\theta_t = 23.0°$ in satisfactory agreement with Table II. Arndt[1] uses this approximation in defining his version of the observables *A0ST*, *KS0T*, *MSNT*, etc.

A difficulty with the additional angle bins of Table III arises with $A_{00n0}$. The Janus polarimeter complicates the measurement of $A_{00n0}$ as follows. The scattered protons have a polarization that depends on the observable $D_{n0n0}$. Protons incident on the right side of Janus scatter toward the center if their spin is up and away from the center if their spin is down, thus changing the effective solid angle as a function of beam spin, and biasing the results for $A_{00n0}$. Events in the central bin are unaffected, but the noncentral bins are biased in opposite directions. We have corrected four values of $A_{00n0}$ as follows: 57.4°: −0.004; 62.3°: +0.004; 67.3°: −0.009; 72.4°: +0.009. These corrections have been added to the uncertainties in Table III.

Systematic normalization uncertainties from the beam and target polarizations and the polarization of the scattered proton are not included in the tables, and must be applied to all the data by multiplying by a renormalization factor. The overall normalization uncertainty for the scattered proton polarization (which applies to all observables with *s*, *n* or *k* in the first subscript) is ±2% as discussed in Ref. 15. The normalization uncertainty for the beam polarization[11] is ±1%, which applies to all observables with *s*, *n*, or *k* in the third subscript. For the target polarization we estimate a normalization uncertainty of ±5% which applies to all observables with *t* as the fourth subscript.

## RESULTS AND CONCLUSIONS

The observables are defined in Table I, listed for the four spectrometer angles in Table II, and rebinned into 12 angles in Table III. Figure 2 illustrates the data in comparison with the phase shifts of Arndt[1] (which include these data) and Bystricky[2] (which do not include these data). Agreement is good, which indicates that these new data are consistent with previous data. This confirms that the nucleon-nucleon isospin-one amplitudes are generally well determined near 730 MeV.

The data presented here form a complete set at 730 MeV, so that the 5 scattering amplitudes[8] can be extracted directly from the data. The 14 observables measured here overdetermine the amplitudes, so the amplitudes were determined by $\chi^2$ minimization, with $\chi^2$ per degree of freedom = 1.1. The amplitudes (normalized to 1) and the phases (relative to the phase of the amplitude *e*) extracted directly from the data are compared with the values extracted from Arndt's[1] and Bystricky's[2] phase-shift solutions in Figs. 3 and 4. Agreement is good, adding further weight to the conclusion that the spin depen-

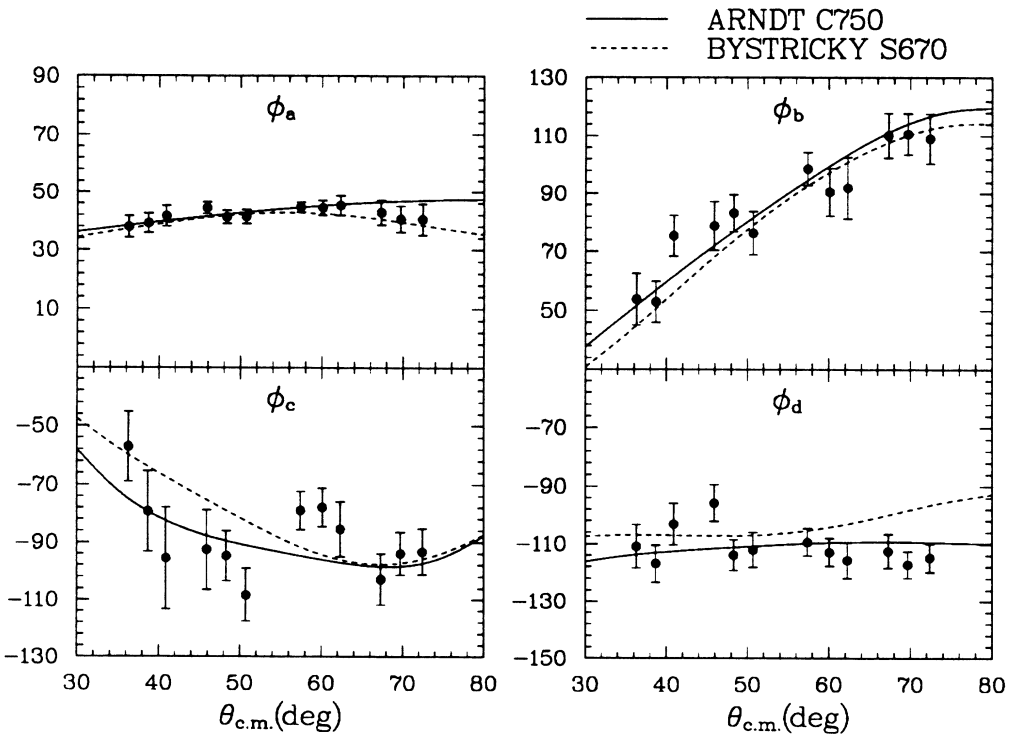


FIG. 4. Phases (relative to the phase of the amplitude *e*) of the *NN* isospin-1 amplitudes; direct reconstructions from the data compared with the phase shifts of Arndt and Bystricky.

dence of $pp$ scattering is well determined.

To summarize, these new data bring the 730-MeV data up to the standard of the data near 500, 580, 650, and 800 MeV. The spin dependence of $pp$ scattering is generally well determined at intermediate energies. Completion of the isospin-one data set awaits the publication of the precise (1%) absolute cross-section data recently measured at LAMPF.

---

*Present address: Rice University, Houston, Texas 77251.

†Present address: DPhPE, CEN Saclay, 91191 Gif-sur-Yvette CEDEX, France.

‡Present address: Los Alamos National Laboratory, Los Alamos, New Mexico 87545.

[1]R. A. Arndt, L. D. Roper, R. A. Bryan, R. B. Clark, B. J. VerWest, and P. Signell, Phys. Rev. D **28**, 97 (1983).

[2]J. Bystricky, C. Lechanoine-Leluc, and F. Lehar, J. Phys. **48**, 199 (1987).

[3]D. V. Bugg (submitted to Phys. Rev).

[4]R. Hausammann *et al.*, Phys. Rev. D **40**, 22 (1989).

[5]M. J. Moravcsik, F. Arash, and G. R. Goldstein, Phys. Rev. D **31**, 1577 (1985).

[6]P. Gonzales and E. L. Lomon, Phys. Rev. D **34**, 1351 (1986).

[7]F. Lehar, in *High Energy Spin Physics (Brookhaven National Laboratory and Westhampton Beach, New York)*, Proceedings of the Fifth High Energy Spin Symposium, AIP Conf. Proc. No. 95, edited by G. Bunce (AIP, New York, 1983), p. 191.

[8]J. Bystricky, F. Lehar, and P. Winternitz, J. Phys. **39**, 1 (1978).

[9]*Proceedings of Workshop on Higher Energy Polarized Beams, (Ann Arbor, 1977)*, Proceedings of the Workshop on Higher Energy Polarized Beams, AIP Conf. Proc. No. 42, edited by A. D. Krisch and A. J. Salthouse (AIP, New York, 1977), p. 142.

[10]R. Ransome, S. J. Greene, C. L. Hollas, B. E. Bonner, M. W. McNaughton, C. L. Morris, and H. A. Thiessen, Nucl. Instrum. Methods **201**, 309 (1982).

[11]M. W. McNaughton and E. P. Chamberlin, Phys. Rev. C **24**, 1778 (1981).

[12]M. W. McNaughton, Los Alamos National Laboratory Report No. LA-11670-PR (1989), p. 164.

[13]M. W. McNaughton *et al.*, Phys. Rev. C **25**, 1967 (1982).

[14]C. L. Hollas *et al.*, Phys. Rev. C **30**, 1251 (1984).

[15]M. W. McNaughton *et al.*, Nucl. Instrum. Methods **A241**, 435 (1985).